1521-009X/50/3/268–276$35.00
DRUG METABOLISM AND DISPOSITION

dx.doi.org/10.1124/dmd.121.000751
Drug Metab Dispos 50:268–276, March 2022

Antisense Oligonucleotide In Vitro Protein Binding Determination in Plasma, Brain, and Cerebral Spinal Fluid Using Hybridization LC-MS/MS[S]

Guilherme Guimaraes, Long Yuan,* and Pei Li

Drug Metabolism and Pharmacokinetics, Biogen, Cambridge, Massachusetts

Received October 28, 2021; accepted December 10, 2021

ABSTRACT

The development of quantitative models for prediction of drug pharmacokinetics based on in vitro data has transformed early drug discovery. Drug unbound fraction (f_u) characterization is a key consideration in pharmacokinetic and pharmacodynamic (PK/PD) modeling, assuming only unbound drug can interact with the target, and therefore has direct implications in the efficacy and potential toxicity of the drug. The current study describes the implementation of a hybridization liquid chromatography–tandem mass spectrometry (LC-MS/MS) platform for the direct quantitation of antisense oligonucleotide (ASO) f_u. The method provides substantial improvements, including minimal matrix effects and high specificity when compared with previously used oligonucleotide f_u detection methods such as ligand binding assays or liquid scintillation. The hybridization LC-MS/MS platform was integrated with ultracentrifugation, ultrafiltration, and equilibrium dialysis, and method performance for each technique was evaluated. Although ASO protein binding has been previously characterized in plasma, there were no studies that quantitated ASO f_u in brain or cerebral spinal fluid (CSF). As ASOs continue to undergo clinical trials for neurologic and neuromuscular indications, f_u characterization in brain and CSF can provide invaluable information about ASO distribution and target engagement in the central nervous system, therefore providing support for in vivo PK/PD data characterization.

SIGNIFICANCE STATEMENT

A novel hybridization LC-MS/MS-based approach was successfully developed for the determination of ASO in vitro protein binding in plasma, and for the first time brain and CSF. Ultrafiltration, equilibrium dialysis, and ultracentrifugation were assessed for the separation of unbound ASO from biological matrices. The hybridization LC-MS/MS platform provided unique advantages, including minimal matrix effects and high specificity, compared with traditional ligand binding assays or liquid scintillation approaches, which enabled efficient and reliable in vitro protein binding assay.

Introduction

Antisense oligonucleotides (ASOs), defined as short synthetic oligonucleotides with single-stranded sequences complementary to certain mRNA sites, have been under drug development for approximately 30 years, with the first FDA-approved drug, Fomivirsen, being approved in 1998 (Stein and Castanotto, 2017). Chemical modifications such as substitution of one nonbridging oxygen (phosphate) for a sulfur (phosphorothioate) have increased stability against nuclease degradation as well as plasma protein binding, with phosphorothioated oligonucleotides being highly protein bound (>85%) (Levin et al., 2007; Geary et al., 2015). Proper characterization of ASO's chemical modifications and its biologic ramifications are important, as ASO pharmacokinetic properties are largely driven by chemistry rather than sequence (Geary et al., 2001; Geary et al., 2015).

Drug unbound fraction (f_u) quantification in any given matrix is essential in understanding drug pharmacokinetics, as it is generally accepted that only the unbound drug is available and responsible for drug efficacy and potential drug toxicity (Rowland et al., 2011; Mariappan et al., 2013; Roberts et al., 2013). f_u quantification provides valuable insight into drug absorption, distribution, metabolism, excretion, and toxicity. Although ASO f_u has been previously characterized in plasma, ASO f_u in matrixes of high interest such as brain and cerebral spinal fluid (CSF) is still unknown. Owing to relatively large molecular size and multiple negative charges, ASOs do not efficiently cross the blood-brain barrier (Geary et al., 2015; Bennett et al., 2017). However, this limitation has been mitigated through intracerebroventricular or intrathecal delivery while less invasive delivery techniques continue to be developed (Miller et al., 2013; Wurster and Ludolph, 2018; Alarcón-Arís et al., 2020; Min et al., 2020). To better understand ASO exposure and target occupancy in the CNS, proper f_u characterization in brain and CSF is crucial.

Historically, f_u determination for small-molecule drug candidates has been determined by ultrafiltration, ultracentrifugation, or equilibrium dialysis, which are techniques based on the physical separation of unbound drug molecules from those bound to proteins (Pacifici and Viani, 1992). In vitro drug f_u results are one of the properties used to prioritize certain drug candidates into further stages of drug development. Owing to their physical properties, such as relatively high molecular weight, linear structure, and nonspecific binding, ASOs present unique challenges in f_u determination through traditional techniques. Because of the linear conformation of ASOs, the molecular weight cutoff (MWCO) for dialytic membranes needs to be much higher than the

dx.doi.org/10.1124/dmd.121.000751.
[S] This article has supplemental material available at dmd.aspetjournals.org.

ABBREVIATIONS: ACSF, artificial cerebral spinal fluid; ASO, antisense oligonucleotide; CSF, cerebral spinal fluid; f_u, unbound fraction; LC-MS/MS, liquid chromatography–tandem mass spectrometry; MW, molecular weight; MWCO, molecular weight cutoff; NSB, nonspecific binding; PK/PD, pharmacokinetic and pharmacodynamic; RED, rapid equilibrium dialysis.

ASO molecular weight (generally ~7 kDa). The lack of commercially available equilibrium dialysis membranes with MWCO over 20K makes this technique incompatible with ASOs (Rocca et al., 2019). Ultrafiltration also requires a membrane medium, which becomes a major source for oligonucleotide nonspecific adsorption and therefore low recoveries. To overcome this issue, membrane pretreatment with surfactants or sacrificial oligonucleotides that are irrelevant to the analyte have shown to provide acceptable recoveries (Watanabe et al., 2006; Humphreys et al., 2019). Ultracentrifugation bypasses the need for a membrane; however, low recoveries have been reported for siRNA, potentially owing to differential sedimentation of macromolecules (Hughes et al., 1938; Humphreys et al., 2019). Alternatively, electrophoretic mobility shift has been evaluated as a method for determining siRNA f_u in plasma (Rocca et al., 2019). Although this technique also bypasses the need for a membrane, limited sample throughput prevents it from being widely applied in drug discovery.

Previous detection methods for oligonucleotide f_u determination included liquid scintillation and hybridization techniques such as real-time PCR. There are several advantages when choosing liquid chromatography–tandem mass spectrometry (LC-MS/MS) over previous methods, including the generation of more quantitative values, easier normalization, and less biased results coming from different variations of PCR techniques (Wang et al., 2013; Basiri et al., 2019). Additionally, liquid scintillation requires the synthesis of radiolabeled ASOs that are expensive to produce and challenging to dispose of.

In this work, ASO f_u in plasma, brain, and CSF were characterized through an ultrafiltration hybridization LC-MS/MS platform. This is the first time LC-MS was used for direct quantitation of ASO f_u in not only plasma, but also brain tissue and CSF, for a more complete understanding of ASO protein binding. The method allowed specific and sensitive analysis, wide linear range, and automation of the hybridization extraction (Li et al., 2020). Complete elimination of matrix effects enabled the direct comparison between unbound and bound ASO in different sample compositions, which was otherwise unachievable by previous methods. In addition to ultrafiltration, equilibrium dialysis and ultracentrifugation were also evaluated, although membrane incompatibility, limited sample throughput, and sampling bias hinders their performance. f_u was characterized for three different ASOs across different matrixes in multiple species.

Materials and Methods

Materials. Analyte ASO-1, ASO-2, ASO-3, and the internal standard (ASO-4) were proprietary assets of Biogen and provided by its collaborator, with basic information shown in Table 1. Capture probes (biotinylated reverse complimentary DNA) were synthesized by Integrated DNA Technologies (Coralville, IA). Rapid equilibrium dialysis (RED) device (12 kDa MWCO), Pierce BCA protein assay kit, Dynabeads MyOne streptavidin C1, and RNA grade proteinase K solution (20 mg/ml) were purchased from Thermo Fisher Scientific (Waltham, MA). Clarity OTX lysis-loading buffer was acquired from Phenomenex (Torrance, CA). Amicon Ultra 0.5-ml centrifugal filters (10, 30, 50, and 100 kDa MWCO), Trizma base, sodium chloride, Tween-20, and ethylenediaminetetraacetic acid were acquired from MilliporeSigma (St. Louis, MO). 1,1,1,3,3,3-Hexafluoro-2-methyl-2-propanol was obtained from Alfa Aesar (Tewksbury, MA). N,N-dimethylcyclohexylamine was obtained from TCI America (Portland, OR). HPLC-rade acetonitrile (ACN) and DL-1,4-dithiothreitol (DTT) were obtained from Fisher Scientific (Hampton, NH). Pooled rat, mouse, dog, monkey and human plasma (K2EDTA) as well as male rate brain homogenate and monkey CSF were obtained from BioIVT (Westbury, NY). Artificial cerebral spinal fluid (ACSF) was acquired from Tocris Bioscience (Minneapolis, MN). Biogen in-house Milli-Q deionized water was used.

Ultrafiltration. A volume of 0.5 ml PBS (0.137M NaCl, 0.0027M K, 0.0119M phosphates) with 0.1% Tween-20 (v/v; PBST) was added to Amicon Ultra 0.5-ml centrifugal three times to remove residual glycerin and condition filter. Following every PBST addition, 30-, 50-, and 100-kDa filters were spun in a bench-top centrifuge for 10 minutes at 3000 × g, whereas 10 kDa-filters were spun at 5000 × g. After the third addition of PBST, filters were incubated at room temperature for 15 minutes before centrifugation. Any residual treatment solution was removed, whereas the collection tube was retained. For the sample treatment experiment, four conditions were evaluated: 0.1% Tween-20 in PBS, 5 μM sacrificial ASO in PBS, 5 μM sacrificial ASO in PBS with 1% Tween-20, and 5 μM sacrificial ASO in PBS with 0.1% Tween-20. Spiked matrixes were added to filters immediately after treatment to ensure filters never dried out. For recovery experiments, 1 μM ASO-1, 1 μM warfarin and 1 μM antipyrine were co-spiked into PBS. A volume of 0.5 ml was transferred to treated filters and incubated at room temperature for 15 minutes. Following incubation, 10-kDa MWCO filters were centrifuged at 3000 × g for 1 minute, whereas 30-, 50-, and 100-kDa filters were centrifuged at 1500 × g. Centrifugation time varied for different matrixes and filter MWCO sizes.

Plasma (preequilibrated to 37°C) was co-spiked with 1 μM ASO, 1 μM warfarin, and 1 μM antipyrine and incubated at 37°C while shaking at 500 rpm. 500 μl of spiked plasma was transferred to treated filters and 10-kDa MWCO filter centrifuged at 3000 × g for 2 minutes, whereas 30-, 50-, and 100-kDa centrifuged at 1500 × g for the same amount of time. The same procedure was repeated for brain homogenate and CSF samples, but centrifugation time varied between matrixes: brain homogenate, 10 kDa (3000 × g) and 30, 50, and 100 kDa (1500 × g) for 3 minutes; CSF, 10 kDa (3000 × g), and 30, 50, and 100 kDa (1500 × g) for 2 minutes. Centrifugation time and speed were optimized to ensure sufficient but no more than 20% of the sample crossed the filter. CSF was also co-spiked with 1 μM ASO, 1 μM warfarin, and 1 μM antipyrine, whereas brain homogenate was co-spiked with 1 μM ASO and 1 μM verapamil. Ultracentrifugation and rapid equilibrium dialysis methods, as well as the small-molecule LC-MS/MS quantification method, are provided in the Supplemental Material.

ASO Quantification. For ASO quantification, 10 μl of the filtered (representing "free") or unfiltered (representing "total") sample was combined with 90 μl of corresponding blank matrix in a Kingfisher 96 deep-well plate (Thermo Fisher Scientific, Waltham, MA). Sample preparation and LC-MS/MS analysis were conducted following a previously published protocol from Li and coworkers with minor modifications (Li et al., 2020). Multiple reaction monitoring transitions used were: ASO-1 (785→94.9 m/z), ASO-2 (637.7→94.9 m/z), ASO-3 (660.1→94.9 m/z).

Recovery and f_u were calculated as previously described by Humphreys and coworkers using the following equations:

$$\%\ Recovery\ (buffer)\ =\ \frac{[receiver]}{[donor]}\ X\ 100 \tag{1}$$

$$f_u = \frac{[receiver]}{[donor]} \tag{2}$$

where [donor] is the original concentration of drug in the spiked matrix prior to addition to filtration apparatus, and [receiver] is the drug concentration in the ultrafiltrate (Humphreys et al., 2019).

TABLE 1

ASO analytes and internal standard

Name	MW (kDa)	Sequence Length	Chemistry	Use
ASO-1	7.1	20	5 − 10−5 MOE-gapmer	analyte
ASO-2	7.1	20	5 − 10−5 MOE-gapmer	analyte
ASO-3	5.9	17	MOE/cEt-gapmer	analyte
ASO-4	7.9	20	uniform MOE with PS backbone	internal standard

cEt, constrained ethyl motif; MOE, 2′-O-(2-methoxyethyl)-oligoribonucleotides; PS, phosphorothioate linkage.

In this study, f_u is shown in terms of percentage, meaning that eq. 2 is multiplied by 100. Lastly, the dilution for brain homogenate (1:8) was adjusted through the following equation described by Kalvass and coworkers (Kalvass and Maurer, 2002; Kalvass et al., 2007):

$$undiluted\ f_u = \frac{1/D}{[(1/f_{u,\ measured}) - 1]\ +\ 1/D} \quad (3)$$

D represents the dilution factor of brain tissue, and $f_{u,measured}$ is the ratio described in eq. 2. All ultrafiltration and RED experiments had a minimum number of 3 replicates ($N \geq 3$). Owing to limited throughput, ultracentrifugation experiments were not replicated ($N = 1$).

Results

Recovery Evaluation

To assess analyte nonspecific binding (NSB) to the filter membrane, the major potential limitation of ultrafiltration, recovery was evaluated for different filter pretreatment conditions and different filter sizes by measuring the percentage of drug remaining in a protein-free medium after filtration (Toma et al., 2021). Recovery determination was calculated through eq. 1. Fig. 1A shows the recovery of 1 μM ASO-1 in PBS under five different filter treatment conditions, including untreated (filter rinsed with PBS), 0.1% Tween-20 in PBS, 5 μM sacrificial ASO in PBS, 5 μM sacrificial ASO in PBS with 1% Tween-20, and 5 μM sacrificial ASO in PBS with 0.1% Tween-20. Recovery was assessed in 30K MWCO filters, which was the size showing significant but mitigatable loss to NSB. Consistent with previous reports, filter pretreatment with either Tween-20 or sacrificial ASO was shown to minimize NSB (Watanabe et al., 2006; Humphreys et al., 2019). Based on recovery against a commonly accepted criterion at 80%, 0.1% and higher concentrations of Tween-20, with or without the combination of sacrificial ASO, provided sufficient anti-NSB protection, suggesting 0.1% Tween-20 to be the ideal blocking agent. Previous studies have shown Tween-20 to be the best blocking agent over several conditions, including heparin, irrelevant oligonucleotides, bovine serum albumin, and others (Humphreys et al., 2019; Rocca et al., 2019).

Upon determining optimal filter treatment with 0.1% Tween-20, recovery of 1 μM ASO-1 co-spiked with 1 μM warfarin and antipyrine was evaluated at four different filter MWCO sizes (Fig. 1, B and C). Although low recovery was observed for 10K filters, acceptable recovery was achieved for 30, 50, and 100K MWCO filters, suggesting a correlation between recovery and MWCO and further suggesting that unbound ASO cannot effectively pass 10K filter owing to size constraint. MWCO of membranes is determined based upon a relationship between molecular weight and globular size as defined by Humphreys and co-workers (Humphreys et al., 2019). Given this relationship, the linear nature of oligonucleotides requires much higher MWCO, even though the molecular weight (MW) of ASOs in this study was below 10 kDa (Humphreys et al., 2019). Although filter size and treatment have direct implications on ASO recovery, these variables have no apparent impact on the recovery of small molecule controls (Fig. 1C), confirming that the filter size had no impact on drug molecules that were significantly smaller than the MWCO. In summary, conditions of MWCO above 30K and treatment with 0.1% Tween-20 were considered sufficient in ensuring unbound ASO recovery. Recovery of 83% was observed at 30K MWCO in comparison with 96% recovery at 50K and 100K MWCO.

ASO f_u Determination in Plasma

Plasma f_u experiments were conducted at all filter sizes (Fig. 2A), and experiments were orthogonally validated through co-spiked small molecules that are either highly protein bound (warfarin) or highly protein unbound (antipyrine). As filter MWCO increased, measured plasma f_u also increased for both ASO and small-molecule controls. The upward trend suggests protein bleeding, specifically for proteins carrying bound drug molecules, in larger MWCO filter sizes as the responsible factor for artificially higher plasma f_u measurements. In the

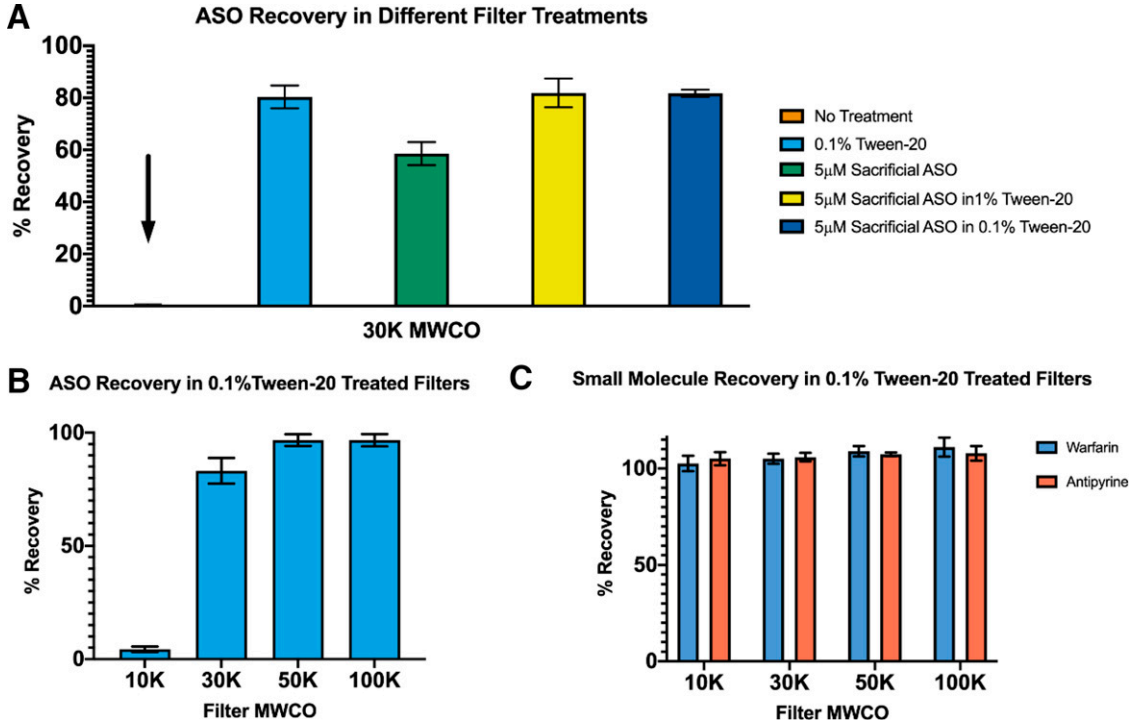

Fig. 1. (A) Recovery of 1μM ASO-1 in PBS through different filter pretreatments. (B) Recovery of 1μM ASO-1 in different MWCO filter sizes pre-treated with 0.1% Tween-20 (PBST). (C) Recovery of 1μM warfarin and antipyrine in different MWCO filter sizes pretreated with 0.1% Tween-20 (PBST).

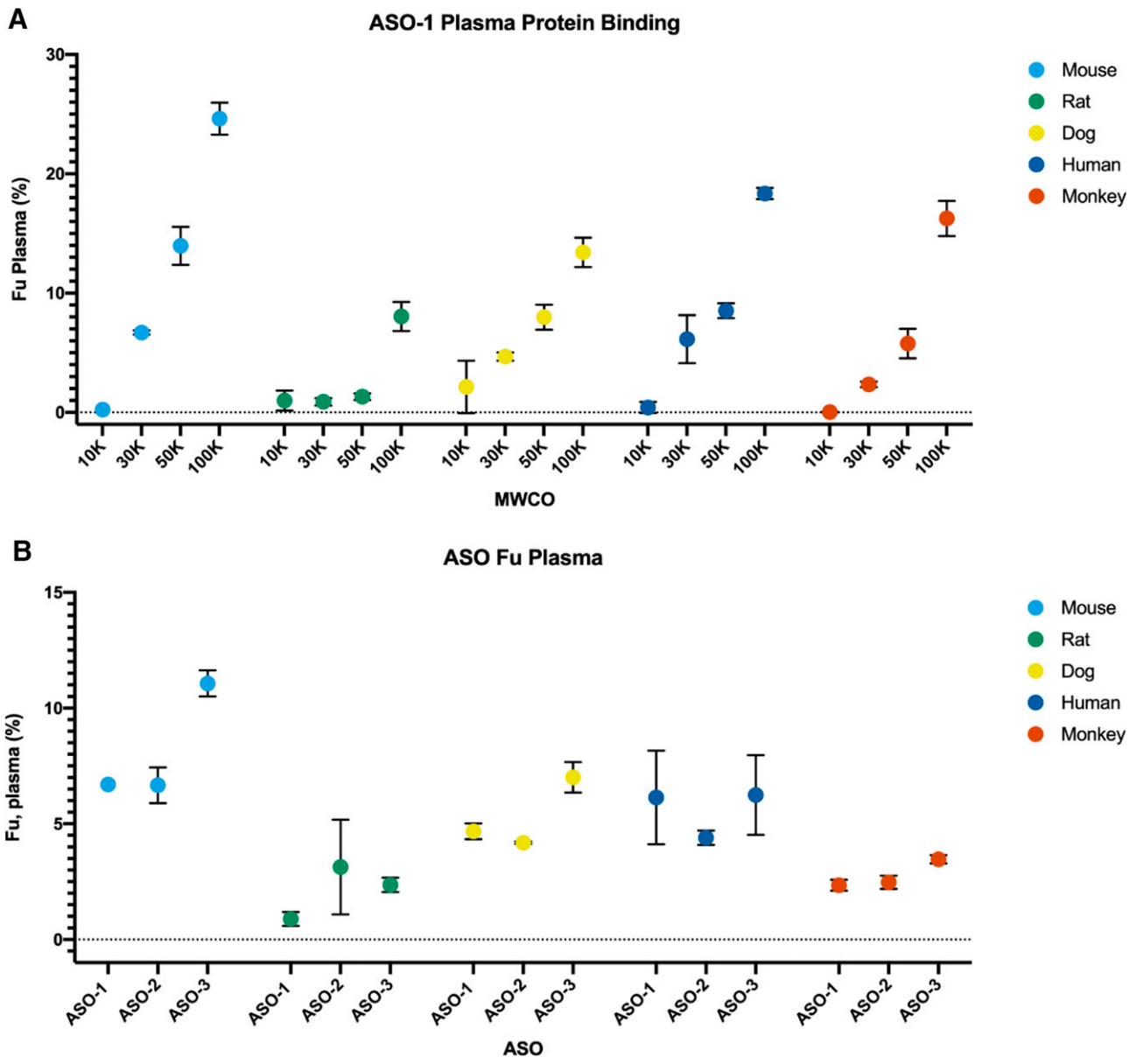

Fig. 2. (A) ASO-1 plasma fu in different MWCO filter sizes. (B) ASO-1, ASO-2, and ASO-3 plasma fu in 30K MWCO filters.

context of this study, protein bleeding is defined as proteins with higher MW than filter cutoff or proteins carrying bound drug molecules that pass through the filter and end up in the ultrafiltrate. Previous studies have shown ASOs to be highly bound to albumin (Cossum et al., 1993; Srinivasan et al., 1995; Watanabe et al., 2006). Albumin has a relatively low MW (~66.5 kDa) and has been identified in the ultrafiltrate of a 50K MWCO ultrafiltration assay through electrophoretic mobility, suggesting protein bleeding even though the MW is higher than the MWCO (Humphreys et al., 2019). Similarly, warfarin is also highly bound to albumin, and its concentration in the ultrafiltrate is also artificially higher when using 50K or higher MWCO filters, which results in a similar upward trend to those observed in Fig. 2A (Supplemental Fig. 1A). In contrast, minimal change in antipyrine concentration in the ultrafiltrate was observed in different MWCO filters, as it is highly unbound and not significantly affected by protein bleeding (Supplemental Fig. 1B). To minimize the impact of protein bleeding, the smallest filter size that still achieved satisfactory recovery, in this case 30K MWCO, was chosen as the final condition. Plasma f_u measurements were repeated in two other ASOs across five species (Fig. 2B). Interspecies differences in plasma f_u were observed following a trend in the order of rat < monkey < human ≈ dog < mouse, which was consistent with previously reported results (Watanabe et al., 2006). In addition, Watanable and coworkers described an inverse relationship between ASO sequence length and unbound concentration through plasma f_u measurements of 10 shortmer metabolites. Although plasma f_u for ASO metabolites was not evaluated in this study, higher unbound concentrations were observed for ASO-3 (17mer) in comparison with the other two ASOs (20mers). The 30-kDa MWCO ultrafiltration method was orthogonally validated through previously characterized small-molecule controls, shown in Table 2. The results

TABLE 2

Orthogonal validation of 30 kDa MWCO ultrafiltration method through previously characterized small molecules

	Experimental Values (%)	Experimental Values Generated Using a Standard RED Protocol (%)	LiteratureValues (%)
		Plasma	
Warfarin			
Mouse	5.5 ± 0.3	4.3 ± 0.9	4.6 ± 0.4[a]
Rat	1.0 ± 0.5	0.8 ± 0.4	1.1[b]
Dog	3.2 ± 0.1	3.9 ± 0.7	4.0 ± 0.1[a]
Human	1.1 ± 0.5	1.5 ± 0.3	1.0[c]
Monkey	0.8 ± 0.2	1.0 ± 0.7	0.7 ± 0.1[a]
Antipyrine			
Human	92.8 ± 2.2		90[d]
		Brain	
Verapamil			
Rat	2.8 ± 0.3	3.8 ± 1.4	3.3 ± 2.0[e]

[a]Isbell et al., 2019.
[b]Hirate et al., 1990.
[c]Zhang et al., 2012.
[d]Humphreys et al., 2019.
[e]Hirate et al., 1990.

generated from the ultrafiltration method were consistent with those from standard RED methods, as well as the literature-reported values. This further demonstrated the validity of the developed ultrafiltration method.

ASO f_u Determination in Brain Tissue Homogenate

Ultrafiltration experiments were similarly conducted in rat brain tissue homogenate. ASO f_u determination at 1 μM was orthogonally validated through co-spiked 1 μM verapamil, a better characterized compound for brain f_u. Brain f_u determination was carried out at four different MWCO sizes, across three different ASOs. As seen in Fig. 3, similar upward trend in measured brain f_u was observed as filter sizes increased, suggesting protein bleeding to influence measured brain f_u. Just like in plasma samples, the most suitable filter size was 30 kDa MWCO. Overall, rat brain f_u was sevenfold lower in comparison with rat plasma f_u. Differences in f_u in brain homogenate in comparison with plasma f_u are likely owing to differences in protein concentration in the two matrices. The correlation between higher protein content and higher protein binding has been discussed by Liu and coworkers (Liu et al., 2014). Based on this correlation, lower brain f_u is likely owing to the brain's higher protein content in comparison with protein content in plasma.

ASO f_u in CSF

The final biologic matrix in which ASO f_u was characterized was monkey CSF. As expected, CSF f_u was significantly higher in comparison with other biologic matrices owing to its relatively low protein composition. Initially, protein binding experiments were carried out in CSF and protein-free ACSF. Fig. 4A showed ASO-1 f_u in CSF and ACSF in different filter sizes. ACSF protein binding results were similar to recovery experiments, as both ACSF and PBS are protein-free. Differences between 30K and 50K filters in CSF were proportional to differences between these sizes in ACSF. Furthermore, 30K CSF f_u values can be corrected in accordance with differences in recovery between 30K and 50K filters in ACSF. The f_u corrected is similar to f_u in 50K filters (Supplemental Fig. 2), suggesting that protein bleeding is less concerning in CSF, likely owing to its relative low protein composition.

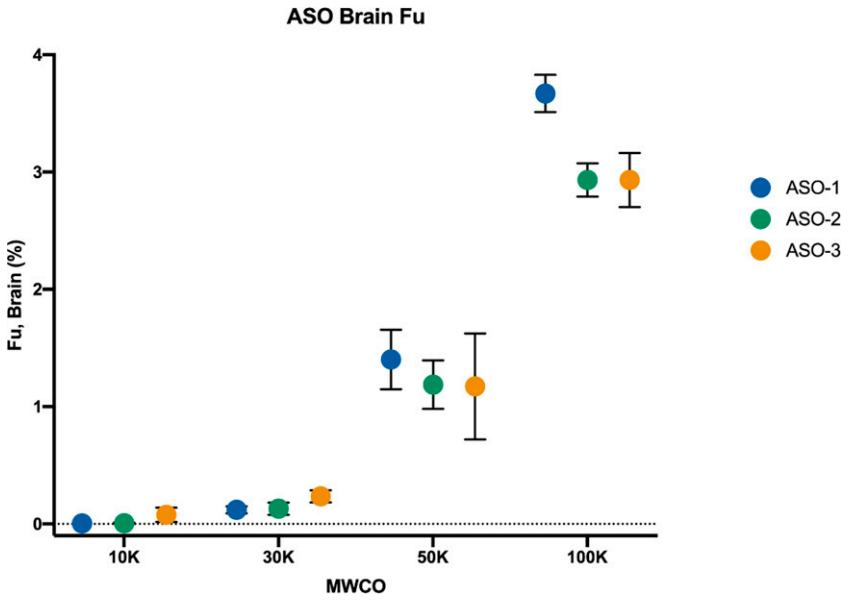

Fig. 3. ASO brain fu across different filter sizes.

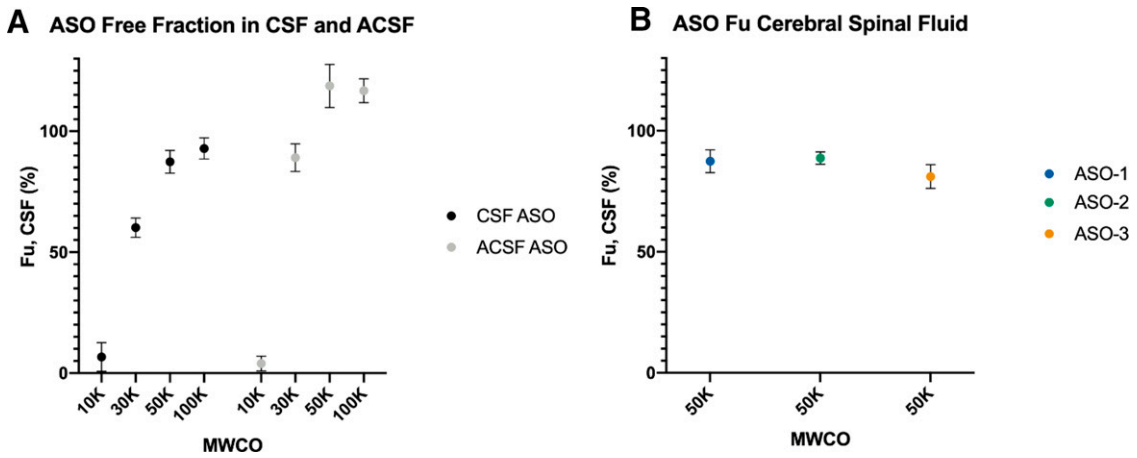

Fig. 4. (A) ASO-1 drug unbound fraction in CSF and artificial CSF. (B) ASO CSF unbound fraction in 50K MWCO filters.

Overall, these results suggested that 50K filters were the appropriate size for CSF f_u quantification without the need for recovery normalization. CSF f_u for different ASOs was quantified in 50K MWCO filters (Fig. 4B). Co-spiked warfarin and antipyrine CSF and ACSF f_u is available in Supplemental Fig. 3. Similar to warfarin f_u in plasma and brain homogenate, there is an upward trend in CSF f_u as the filter MWCO increases, which can be attributed to protein bleeding. However, warfarin CSF f_u measurements were not significantly different between 30K and 50K MWCO filters, owing to the low concentrations of CSF proteins within this narrow MW range, and therefore limited impact from protein bleeding. For antipyrine, owing to its highly unbound nature, filter size had no impact on CSF f_u measurements.

Equilibrium Dialysis. RED is a popular technique for high throughput protein binding assays and often referred to as the "gold standard" (Trainor, 2007). As previously shown, filter MWCO plays a key role in ASO recovery. The first step in RED was to confirm if ASO concentrations both in the sample compartment and solvent compartment reached equilibrium in a protein-free medium. Despite different membrane pretreatments and prolonged incubations, system equilibrium was never reached with the biggest available MWCO at 12K, suggesting ASOs were not physically able to cross the membrane limited by the pore size. Results were also comparable to poor ASO permeability of similar MWCO at 10K demonstrated in the ultrafiltration section. Both small-molecule controls (warfarin and antipyrine) reached equilibrium under the assessed experimental conditions (Fig. 5), which not only orthogonally confirmed the validity of the experiment, but also pointed the loss of ASO to its higher MW and unique NSB.

Ultracentrifugation

In addition to ultrafiltration and RED, an ultracentrifugation method was explored, and its compatibility with ASOs was assessed. Polycarbonate tubes were filled with either 1 ml of rat plasma or PBS, co-spiked with 1 μM ASO-1 and 1 μM warfarin. Spiked samples were centrifuged at 400,000 × g for 1, 2, 3, and 4 hours. Upon collection of each time point, a 1-ml sample was divided into four vertical quadrants of equal volumes (250 μl each), with the top layer (first 250 μl) being "Q1", second 250 μl being "Q2" and so on. ASO-1 and warfarin concentrations were quantified for every quadrant, and their recoveries were calculated against precentrifuge samples and shown in Table 3. Protein concentration for different quadrants is shown in Supplemental Table 1.

Similar to ultrafiltration, analyte recovery was first assessed in PBS and confirmed that there was no significant loss of ASO-1 or warfarin to the experimental system without the impact of any protein binding. It was noticed that ASO-1 quickly formed a concentration gradient 74.3–153.5% from Q1 to Q4 at 1 hour and maintained the similar gradient to the end, which was not observed in warfarin. Warfarin initially formed a concentration gradient in PBS (potentially owing to poor solubility and insufficient mixing), but equilibrium between the quadrants was observed in Hours 3 and 4 as expected for a small molecule. The concentration gradient observed for ASO suggested that the relatively higher MW of ASO compared with small molecules led to slight precipitation of unbound ASO at such strong ultracentrifugation conditions, though approximately 80% recovery might still be considered acceptable.

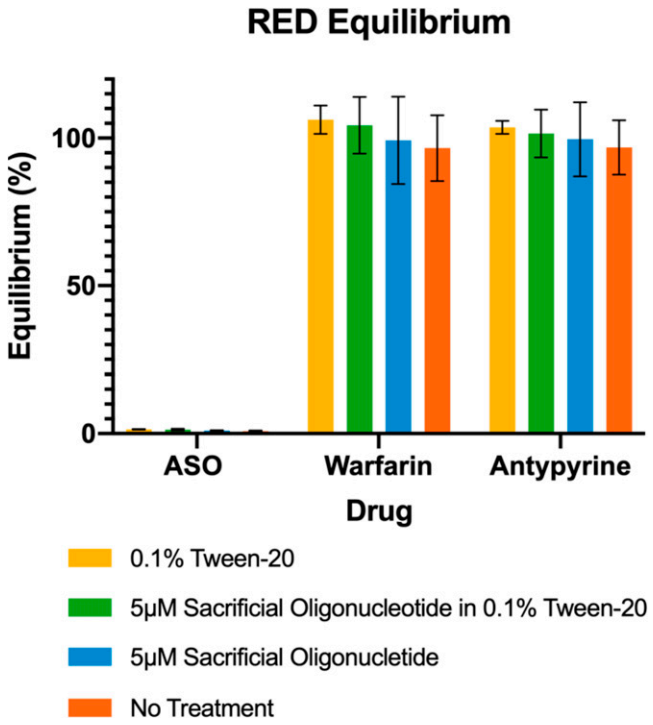

Fig. 5. RED system equilibrium through different membrane pretreatments.

TABLE 3

Ultracentrifugation plasma f_u and recovery in PBS values for ASO-1 and warfarin ($n = 1$)

	Plasma f_u (%)							
	ASO-1				Warfarin			
	1 h	2 h	3 h	4 h	1 h	2 h	3 h	4 h
Q1	14.3	3.4	2.6	2.0	15.7	0.5	0.6	0.6
Q2	63.0	10.7	3.8	2.9	90.8	6.2	0.7	0.5
Q3	122.7	160.7	55.4	58.6	150.0	195.7	71.1	82.2
Q4	204.8	244.5	NA	NA	169.2	184.4	NA	NA
Total recovery	101.2	104.8	NA	NA	106.4	96.7	NA	NA
	Recovery in PBS (%)							
	ASO-1				Warfarin			
	1 h	2 h	3 h	4 h	1 h	2 h	3 h	4 h
Q1	74.3	75.2	78.5	82.5	62.5	73.0	109.1	106.1
Q2	97.9	77.7	79.6	80.1	77.8	72.4	107.5	104.0
Q3	87.7	85.9	84.1	101.2	79.0	76.1	111.9	107.8
Q4	153.5	152.0	110.9	129.5	210.2	216.8	107.5	119.5
Total recovery	103.4	97.7	88.3	98.3	107.4	109.6	109.0	109.4

NA: Recovery was unmeasurable owing to solidified Q4 matrix after ultracentrifugation.

In plasma samples, significant vertical gradients were observed for both ASO-1 and warfarin, owing to the precipitation of protein-bound analytes as expected. After hours, the solution system started to reach equilibrium, in which Q1 was considered protein free as confirmed by total protein quantitated at approximately 0.4% of original. Therefore, ASO-1 rat plasma f_u was determined to be 2.0% based on the Q1 concentration at 4 hours, which was twofold higher than the f_u determined through ultrafiltration (0.89%). Warfarin plasma f_u was measured at 0.6%, lower in comparison with ultrafiltration experiments (1%) and literature (1.1%). Such different directions of bias between ASO and warfarin made it difficult to interpret the results from a systematic perspective. Considering a few facts that *1*) the experiment was not strictly validated by co-spiked warfarin; *2*) unbound ASO also forms a concentration gradient under high centrifugal forces; *3*) measured ASO f_u was higher than references; and *4*) the procedure suffered from low throughput and therefore limited replicates ($n = 1$), the approach of ultracentrifugation was deemed impractical for ASO f_u measurement.

Discussion

The current study assessed ultrafiltration, ultracentrifugation, and equilibrium dialysis to measure ASO f_u in plasma, brain homogenate, and CSF, while successfully implementing LC-MS/MS as a sensitive and direct quantitation method. This is the first time LC-MS/MS has been used for quantification of ASO in vitro protein binding and the first time ultracentrifugation and equilibrium dialysis are evaluated for such application.

Hybridization LC-MS/MS Integration. Both the hybridization extraction and LC-MS/MS quantification offer major advantages over previously published methods (Watanabe et al., 2006). On the detection side, MS provides high specificity and simple signal standardization through the implementation of an internal standard. However, one of the typical drawbacks when coupling MS to the analysis of biologic samples is matrix effect, which is defined as the variations in the analyte signal caused by matrix. To minimize the impact of matrix effects, calibration curves are usually prepared in the same matrix as the study samples, which becomes an inefficient process as the number of matrix components grow. In the case of protein binding experiments, matrix interference becomes problematic when measuring separated unbound ASO and total ASO existing in matrices of different compositions (one protein free and the other protein rich), as none of previously available analytical methods were able to completely avoid matrix effects. The adopted hybridization protocol overcomes matrix effect limitations by capturing the desired ASO from the biologic matrix, washing residual matrix through several washes, and finally eluting the analyte in neat solution containing internal standard. Matrix removal allows for cross-matrix quantification, therefore increasing sample preparation efficiency (Li et al., 2020). Owing to the mechanism of hybridization and the need of a specific capture probe, the ultrafiltration-based hybridization LC-MS/MS method is suitable for accurate protein binding assessments of identified lead ASOs, instead of screening large numbers of ASOs as a high-throughput method. Multiple ASOs can be analyzed in a batched manner as long as separate capture probes are used. The hybridization LC-MS/MS platform is robust and compatible with ultrafiltration, RED, and ultracentrifugation experiments.

Ultracentrifugation Limitations. In theory, ultracentrifugation was a promising technique in ASO f_u quantification because it does not require a filter membrane, therefore avoiding ASO NSB to filter apparatus, ASO poor membrane permeability, and protein bleeding. Recently, low recovery, likely owing to sedimentation, was reported in ultracentrifugation of siRNA (Humphreys et al., 2019). However, throughout the ultracentrifugation experiments, we did not observe the same recovery loss, perhaps owing to the lower molecular weight of ASOs (approximately 7 kDa) in comparison with siRNA (approximately 14 kDa). Even though appropriate recovery was observed in the final (4-hour) time point (82.5%), variance from the recoveries in previous time points suggests sampling challenges. The special division of four quadrants was arbitrary and practically difficult by manual pipetting. Another major limitation with ultracentrifugation is sample throughput, as high-speed rotors have limited capacity. In this study, only 10 samples were able to be analyzed per run, largely limiting the number of replicates to reliably make measurements. In addition, ultracentrifuges able to handle speeds over 400,000 × g for multiple hours are not widely available. Because of lower sample throughput, and lower reproducibility, ultracentrifugation was a less ideal choice compared with ultrafiltration.

Ultrafiltration Filter Considerations. Owing to their linear structure, ASOs require MWCO filters that are substantially higher than the ASO's MW. Humphreys and coworkers suggested through a siRNA crystal structure that hydrodynamic radius must be taken into consideration when choosing MWCO filter sizes for molecules of linear conformations (Humphreys et al., 2019). In their study, a 50K MWCO filter had to be used over 30K MWCO filters to achieve appropriate recovery for a GalNAc-conjugated siRNA. Watanable and coworkers report over

85% recovery when using 30K MWCO filters treated with 5 μM irrelevant ASO (not radiolabeled) for the analysis of a 20mer phosphonothioate ASO (Watanabe et al., 2006). These results suggest that double-stranded conformations are more rigid in comparison with single-stranded conformations, and therefore smaller MWCO filters (30K) are compatible with ASOs. When choosing between different MWCO sizes, the main consideration becomes ASO bound to small proteins crossing the filter membrane.

In this study, f_u was determined by eq. 2, but in reality, protein-bound ASOs that cross high-MWCO membranes must be taken into consideration. A more realistic representation would be:

$$f_u = \frac{[receiver]}{[donor]} = \frac{[ASO\ unbound\ in\ ultrafiltrate] + [ASO\ protein\ bound\ in\ ultrafiltrate]}{[donor]} \quad (4)$$

The choice of filter size should be the size at which [ASO protein bound in ultrafiltrate] is the least, whereas [ASO unbound in ultrafiltrate] is recovered as much as possible. For these reasons, 30K filters were chosen in the analysis of protein-rich matrices (brain homogenate and plasma).

Interestingly, our results show that filter size is also matrix dependent. For protein-rich matrixes such as brain homogenate and plasma, significant differences between 30K and 50K filters were observed, but in CSF (low protein concentration), differences between 30K and 50K filters were proportional to their differences in recovery. With this in mind, the filter size that was used for f_u determination in CSF was 50K MWCO, whereas 30K might also be considered when corrected by recovery.

Throughout the ultrafiltration experiments, we noticed occasional outliers likely resulting from defective filters or tube-to-tube variations from the manufacture. All the observed outliers were substantially higher than the average for both ASOs and small molecules. Outliers were removed using Pierce's criterion, which was selected as a predetermined elimination criterion (Ross, 2003). A potential limitation from ultrafiltration experiments is that even when using 30K MWCO filters, it is possible that ASO bound to smaller proteins or biomolecules may pass through the filter and end up in the ultrafiltrate, which is, however, an inevitable scenario for any protein-binding assay based on the molecular weight difference between bound and unbound ASO.

Brain Homogenate and CSF f_u. Development of quantitative models for prediction of drug absorption, distribution, and excretion has transformed early drug discovery. In vivo measurements in many instances are possible, but it requires expensive and complex techniques with low sample throughput, which limits its application in early drug discovery and highlights the importance of in vitro data-based prediction models (Trainor, 2007). Total drug and unbound concentrations in various matrixes, including plasma and brain, provide valuable information about drug pharmacokinetics.

The ratio of total drug concentration in the tissue to total drug concentration in the plasma at steady state (K_p) may be used to predict the extent of tissue distribution (Jones and Rowland-Yeo, 2013). K_p has been previously measured in vivo; however, tissue distribution predictive models based on physicochemical and in vitro binding characteristics can effectively replace in vivo models in early-stage drug discovery (Poulin and Theil, 2002; Rodgers and Rowland, 2007; Poulin, 2015). In the CNS, $K_{p\ (brain,\ plasma)}$ does not always correlate to predicted efficacy. Discrepancies are likely owing to drug nonspecific binding to proteins in the brain. Brain f_u quantification is paramount and must be used as a correction factor for total brain concentration, therefore improving mechanistic PK/PD evaluations (Read and Braggio, 2010). In vivo validation of brain f_u can be difficult to measure, although drug concentration in the CSF has been used as a surrogate method for quantifying brain f_u (Liu et al., 2006; Lin, 2008). Although differences between small molecules and ASOs (high molecular weight and polyanionic character) must be taken into consideration, ASO in vitro protein binding may provide important information on drug potency, distribution, and clearance.

Overall, the ability to modulate protein expression makes ASOs a promising therapeutic modality for the treatment of neurodegenerative diseases, as Alzheimer's disease, Parkinson's disease, Huntington's disease, and amyotrophic lateral sclerosis have been linked to toxic protein accumulation (Bossy-Wetzel et al., 2004; Smith et al., 2006; DeVos and Miller, 2013). Owing to relatively large molecular size and negative charge, ASOs do not efficiently cross the blood-brain barrier, but regardless of this limitation, and through novel delivery methods, ASOs continue to undergo clinical trials for CNS-related diseases (Hammarlund-Udenaes et al., 2008; Bennett et al., 2019; Tabrizi et al., 2019; Leavitt and Tabrizi, 2020). With the exciting progress in ASO treatment of neurologic diseases, this study provides valuable insight into ASO pharmacokinetics in the brain and CSF and can be an invaluable tool in the support and characterization of in vivo PK/PD data.

Authorship Contributions

Participated in research design: Guimaraes, Yuan, Li.
Conducted experiments: Guimaraes, Li.
Performed data analysis: Guimaraes, Li.
Wrote or contributed to the writing of the manuscript: Guimaraes, Yuan, Li.

References

Alarcón-Arís D, Pavia-Collado R, Miquel-Rio L, Coppola-Segovia V, Ferrés-Coy A, Ruiz-Bronchal E, Galofré M, Paz V, Campa L, Revilla R, et al. (2020) Anti-α-synuclein ASO delivered to monoamine neurons prevents α-synuclein accumulation in a Parkinson's disease-like mouse model and in monkeys. *EBioMedicine* **59**:102944.

Basiri B, Sutton JM, Hooshfar S, Byrnes CC, Murph MM, and Bartlett MG (2019) Direct identification of microribonucleic acid miR-451 from plasma using liquid chromatography mass spectrometry. *J Chromatogr A* **1584**:97–105.

Bennett CF, Baker BF, Pham N, Swayze E, and Geary RS (2017) Pharmacology of antisense drugs. *Annu Rev Pharmacol Toxicol* **57**:81–105.

Bennett CF, Krainer AR, and Cleveland DW (2019) Antisense oligonucleotide therapies for neurodegenerative diseases. *Annu Rev Neurosci* **42**:385–406.

Bossy-Wetzel E, Schwarzenbacher R, and Lipton SA (2004) Molecular pathways to neurodegeneration. *Nat Med* **10**:S2–S9.

Cossum PA, Sasmor H, Dellinger D, Truong L, Cummins L, Owens SR, Markham PM, Shea JP, and Crooke S (1993) Disposition of the 14C-labeled phosphorothioate oligonucleotide ISIS 2105 after intravenous administration to rats. *J Pharmacol Exp Ther* **267**:1181–1190.

DeVos SL and Miller TM (2013) Antisense oligonucleotides: treating neurodegeneration at the level of RNA. *Neurotherapeutics* **10**:486–497.

Geary RS, Yu RZ, and Levin AA (2001) Pharmacokinetics of phosphorothioate antisense oligodeoxynucleotides. *Curr Opin Investig Drugs* **2**:562–573.

Geary RS, Norris D, Yu R, and Bennett CF (2015) Pharmacokinetics, biodistribution and cell uptake of antisense oligonucleotides. *Adv Drug Deliv Rev* **87**:46–51.

Hammarlund-Udenaes M, Fridén M, Syvänen S, and Gupta A (2008) On the rate and extent of drug delivery to the brain. *Pharm Res* **25**:1737–1750.

Hirate J, Zhu C, Horikoshi I, and Nagase S (1990) Disposition of warfarin in analbuminemic rats. *Int J Pharm* **65**:149–157.

Hughes TP, Pickels EG, and Horsfall FL (1938) A method for determining the differential sedimentation of proteins in the high speed concentration centrifuge. *J Exp Med* **67**:941–952.

Humphreys SC, Thayer MB, Lade JM, Wu B, Sham K, Basiri B, Hao Y, Huang X, Smith R, and Rock BM (2019) Plasma and liver protein binding of *N*-acetylgalactosamine-conjugated small interfering RNA. *Drug Metab Dispos* **47**:1174–1182.

Isbell J, Yuan D, Torrao L, Gatlik E, Hoffmann L, and Wipfli P (2019) Plasma protein binding of highly bound drugs determined with equilibrium gel filtration of nonradiolabeled compounds and LC-MS/MS detection. *J Pharm Sci* **108**:1053–1060.

Jones H and Rowland-Yeo K (2013) Basic concepts in physiologically based pharmacokinetic modeling in drug discovery and development. *CPT Pharmacometrics Syst Pharmacol* **2**:e63.

Kalvass JC and Maurer TS (2002) Influence of nonspecific brain and plasma binding on CNS exposure: implications for rational drug discovery. *Biopharm Drug Dispos* **23**:327–338.

Kalvass JC, Maurer TS, and Pollack GM (2007) Use of plasma and brain unbound fractions to assess the extent of brain distribution of 34 drugs: comparison of unbound concentration ratios to in vivo p-glycoprotein efflux ratios. *Drug Metab Dispos* **35**:660–666.

Leavitt BR and Tabrizi SJ (2020) Antisense oligonucleotides for neurodegeneration. *Science* **367**:1428–1429.

Levin AA, Yu RZ, and Geary RS (2007*) Basic Principles of the Pharmacokinetics of Antisense Oligonucleotide Drugs*, in *Antisense Drug Technology* (Crooke ST ed) pp 183–216, CRC Press, Boca Raton.

Li P, Gong Y, Kim J, Liu X, Gilbert J, Kerns HM, Groth R, and Rooney M (2020) Hybridization liquid chromatography-tandem mass spectrometry: an alternative bioanalytical method for antisense oligonucleotide quantitation in plasma and tissue samples. *Anal Chem* **92**:10548–10559.

Lin JH (2008) CSF as a surrogate for assessing CNS exposure: an industrial perspective. *Curr Drug Metab* **9**:46–59.

Liu X, Smith BJ, Chen C, Callegari E, Becker SL, Chen X, Cianfrogna J, Doran AC, Doran SD, Gibbs JP, et al. (2006) Evaluation of cerebrospinal fluid concentration and plasma free concentration as a surrogate measurement for brain free concentration. *Drug Metab Dispos* **34**:1443–1447.

Liu X, Wright M, and Hop CECA (2014) Rational use of plasma protein and tissue binding data in drug design. *J Med Chem* **57**:8238–8248.

Mariappan TT, Mandlekar S, and Marathe P (2013) Insight into tissue unbound concentration: utility in drug discovery and development. *Curr Drug Metab* **14**:324–340.

Miller TM, Pestronk A, David W, Rothstein J, Simpson E, Appel SH, Andres PL, Mahoney K, Allred P, Alexander K, et al. (2013) An antisense oligonucleotide against SOD1 delivered intrathecally for patients with SOD1 familial amyotrophic lateral sclerosis: a phase 1, randomised, first-in-man study. *Lancet Neurol* **12**:435–442.

Min HS, Kim HJ, Naito M, Ogura S, Toh K, Hayashi K, Kim BS, Fukushima S, Anraku Y, Miyata K et al. (2020) Systemic brain delivery of antisense oligonucleotides across the blood-brain barrier with a glucose-coated polymeric nanocarrier. *Angew Chem Int Ed Engl* **59**:8173–8180.

Pacifici GM and Viani A (1992) Methods of determining plasma and tissue binding of drugs. Pharmacokinetic consequences. *Clin Pharmacokinet* **23**:449–468.

Poulin P (2015) Drug distribution to human tissues: prediction and examination of the basic assumption in in vivo pharmacokinetics-pharmacodynamics (PK/PD) research. *J Pharm Sci* **104**:2110–2118.

Poulin P and Theil FP (2002) Prediction of pharmacokinetics prior to in vivo studies. 1. Mechanism-based prediction of volume of distribution. *J Pharm Sci* **91**:129–156.

Read KD and Braggio S (2010) Assessing brain free fraction in early drug discovery. *Expert Opin Drug Metab Toxicol* **6**:337–344.

Roberts JA, Pea F, and Lipman J (2013) The clinical relevance of plasma protein binding changes. *Clin Pharmacokinet* **52**:1–8.

Rocca C, Dennin S, Gu Y, Kim J, Chigas S, Najarian D, Chong S, Gutierrez S, Butler J, Charisse K et al. (2019) Evaluation of electrophoretic mobility shift assay as a method to determine plasma protein binding of siRNA. *Bioanalysis* **11**:1927–1939.

Rodgers T and Rowland M (2007) Mechanistic approaches to volume of distribution predictions: understanding the processes. *Pharm Res* **24**:918–933.

Ross SM (2003) Peirce's criterion for the elimination of suspect experimental data. *J Eng Technol* **20**:38–41.

Rowland M, Tozer TN, and Rowland M (2011) *Clinical Pharmacokinetics and Pharmacodynamics: Concepts and Applications*, Wolters Kluwer Health/Lippincott William & Wilkins, Philadelphia.

Smith RA, Miller TM, Yamanaka K, Monia BP, Condon TP, Hung G, Lobsiger CS, Ward CM, McAlonis-Downes M, Wei H, et al. (2006) Antisense oligonucleotide therapy for neurodegenerative disease. *J Clin Invest* **116**:2290–2296.

Srinivasan SK, Tewary HK, and Iversen PL (1995) Characterization of binding sites, extent of binding, and drug interactions of oligonucleotides with albumin. *Antisense Res Dev* **5**:131–139.

Stein CA and Castanotto D (2017) FDA-approved oligonucleotide therapies in 2017. *Mol Ther* **25**:1069–1075.

Tabrizi SJ, Leavitt BR, Landwehrmeyer GB, Wild EJ, Saft C, Barker RA, Blair NF, Craufurd D, Priller J, Rickards H, et al.; Phase 1–2a IONIS-HTTRx Study Site Teams (2019) Targeting huntingtin expression in patients with Huntington's disease. *N Engl J Med* **380**:2307–2316.

Toma C-M, Imre S, Vari C-E, Muntean D-L, and Tero-Vescan A (2021) Ultrafiltration method for plasma protein binding studies and its limitations. *Processes (Basel)* **9**:382.

Trainor GL (2007) The importance of plasma protein binding in drug discovery. *Expert Opin Drug Discov* **2**:51–64.

Wang L, Meng M, and Reuschel S (2013) Regulated bioanalysis of oligonucleotide therapeutics and biomarkers: qPCR versus chromatographic assays. *Bioanalysis* **5**:2747–2751.

Watanabe TA, Geary RS, and Levin AA (2006) Plasma protein binding of an antisense oligonucleotide targeting human ICAM-1 (ISIS 2302). *Oligonucleotides* **16**:169–180.

Wurster CD and Ludolph AC (2018) Antisense oligonucleotides in neurological disorders. *Ther Adv Neurol Disord* **11**:1756286418776932.

Zhang F, Xue J, Shao J, and Jia L (2012) Compilation of 222 drugs' plasma protein binding data and guidance for study designs. *Drug Discov Today* **17**:475–485.

Address correspondence to: Long Yuan, Drug Metabolism and Pharmacokinetics, Biogen, 225 Binney Street, Cambridge, MA 02142. E-mail: long.yuan@biogen.com